



**Environmental  
Science**  
Processes & Impacts

**Adsorption of Aromatic Carboxylic Acids on Carbon  
Nanotubes: Impact of Surface Functionalization, Molecular  
Size and Structure**

Journal:	<i>Environmental Science: Processes &amp; Impacts</i>
Manuscript ID	EM-ART-09-2019-000417.R1
Article Type:	Paper

SCHOLARONE™  
Manuscripts

### **Environmental Significance Statement**

Many emerging contaminants are ionizable and display unique adsorption behaviors. However, how their adsorption affinity and capacity on carbon nanotubes as well as the molecular forces in the solid-liquid interface are affected by their molecular structure and size have not been extensively investigated. Combining the strength of experimental studies with molecular simulation, this study highlights the importance of pH-dependent hydrophobic effect and electrostatic interactions in the adsorption of ionizable compounds. The molecular structure of ionizable compounds affects their adsorption orientation, which in turn affects the significance of different intermolecular forces. The results shed new light on the adsorption of emerging contaminants on environmental surfaces, and their fate and transport in the environment.

1  
2  
3 Adsorption of Aromatic Carboxylic Acids on Carbon Nanotubes: Impact of Surface  
4  
5  
6 Functionalization, Molecular Size and Structure  
7  
8  
9

10  
11 Shifan Li<sup>1</sup>, Iskinder Arsano<sup>2</sup>, Saikat Talapatra<sup>3</sup>, Mesfin Tsige<sup>2</sup>, Xingmao Ma<sup>1,\*</sup>  
12  
13

14  
15  
16  
17 <sup>1</sup> Zachry Department of Civil and Environmental Engineering, Texas A&M University, 3136  
18 TAMU, College Station, TX 77843-3136, USA  
19

20  
21 <sup>2</sup> Department of Polymer Science, University of Akron, Akron, OH, 44325  
22

23  
24 <sup>3</sup> Department of Physics, Southern Illinois University Carbondale, Carbondale, IL, 62901  
25  
26  
27  
28  
29

30  
31 \*Corresponding Author

32  
33 Zachry Department of Civil and Environmental Engineering

34  
35 3136 TAMU

36  
37 Texas A&M University, College Station, TX, 77843

38  
39 Phone: (979) 862-1772

40  
41 Email: [xma@civil.tamu.edu](mailto:xma@civil.tamu.edu)  
42  
43  
44  
45  
46  
47  
48  
49  
50  
51  
52  
53  
54  
55  
56  
57  
58  
59  
60

## Abstract

A large quantity of emerging contaminants are ionizable, and the ionized compounds display different adsorption behaviors than their neutral counterparts. In particular, a strong intermolecular force, the negative charge assisted hydrogen bonding ((-)CAHB) was recently identified, which explains the unusually strong adsorption of negatively charged compounds on carbon nanotubes with oxygen-containing functional groups. However, most previous studies only probed molecules with one benzene ring. The adsorption of ionizable compounds with more than one benzene rings and additional functional groups has not been examined. This study investigated the effect of surface functionalization, molecular size and structure of six aromatic carboxylic acids on their adsorption on multi-walled carbon nanotubes (MWNTs) in batch reactors. In addition, the short-range interactions of the neutral acids with MWNTs were calculated to evaluate the effect of aromaticity and bulkiness. Hydrophobicity and electrostatic interactions dominate the intermolecular forces between ionized contaminants and MWNT surfaces. pH dependent octanol/water partitioning coefficient ( $D_{ow}$ ) is a more precise indicator of the adsorption of ionizable compounds on MWNTs. (-)CAHB is a significant force only for compounds with one benzene ring. Hydroxyl and carboxyl functional groups displayed similar capacity to form (-)CAHB, as indicated by the release of hydroxide ions.

## Key words

aromatic carboxylic acids, multi-walled carbon nanotubes, adsorption, charge assisted hydrogen bonding

## Introduction

Emerging contaminants (EC) such as pharmaceuticals, personal care products and petrochemicals are increasingly detected in the environment.<sup>1</sup> While the concentrations of these ECs are mostly in the ng to  $\mu\text{g/L}$  range, concentrations at the mg/L level have been reported. For example, up to 6.5 mg/L of ciprofloxacin, an antibiotic, has been detected in river water, underscoring their prevalence in the environment and potential health consequences.<sup>2</sup> Many of these compounds contain hydroxyl, carboxyl, amino and other functional groups and are ionizable. Specific conditions for their ionization are governed by the nature of the functional groups and the solution pH. The dissociated ions are typically more hydrophilic than the neutral compounds and therefore have higher solubility in water. As a result, they typically spread farther and faster than their neutral counterparts. Since many of these compounds are hazardous to the environment and human health, a wide range of techniques have been explored to lower their concentrations in the environment, including advanced oxidation, ozonation, membrane filtration and photodegradation.<sup>3</sup> However, adsorption of contaminants on carbonaceous materials remains one of the most investigated technologies for the removal of ECs due to their relatively high removal efficiency and cost effectiveness.<sup>4</sup>

Carbon nanotubes (CNTs) are a group of novel carbon-based nanomaterials that display very high adsorption capacity due to their well-defined structures, uniform surfaces and availability of high energy adsorption sites.<sup>5</sup> The adsorption of neutral organic compounds on CNTs has been extensively studied and their adsorption mechanisms well understood.<sup>6</sup> However, previous studies have shown that different mechanisms are involved in the adsorption of ionizable compounds on CNTs.<sup>7</sup> Kah et al (2017)<sup>8</sup> summarized the possible mechanisms involved in the adsorption of ionizable compounds onto carbon-based materials in a

1  
2  
3 comprehensive review. The specific molecular forces contributing to the adsorption of ionizable  
4  
5 compounds on CNTs depend on the properties of the adsorbate and adsorbent, as well as the  
6  
7 solution chemistry, with solution pH as the most important environmental factor. The relevance  
8  
9 of pH stems from its governing role in the dissociation of ionizable compounds and the  
10  
11 functional groups on CNTs. Hydrophobic effect, hydrogen bonding, and  $\pi$ - $\pi$  interactions all  
12  
13 contribute to the adsorption of ionizable compounds with aromatic rings. However, after the  
14  
15 compounds dissociate, electrostatic forces or electron-based forces, such as cation- $\pi$  interactions  
16  
17 and charge-assisted hydrogen bonding (CAHB), become important.  
18  
19  
20  
21

22           Hydrogen bonding is an important intermolecular force in the adsorption of ionizable  
23  
24 compounds on CNTs. Molecular dynamic simulation was previously employed to investigate the  
25  
26 nature of hydrogen bonding formed between bisphenol A, graphene oxide, and water. The  
27  
28 hydrogen bonding between bisphenol A and graphene oxide facilitated by water appears the  
29  
30 strongest among the six types of hydrogen bonding identified in the system.<sup>9</sup> A recent study also  
31  
32 hypothesized that a unique interaction between multiple  $\pi$ -bond and polarization assisted  
33  
34 hydrogen bonding (PAHB) facilitated by the water clusters contributed to the adsorption of  
35  
36 several ionizable organic compounds on biochar.<sup>10</sup> While the significance of this new interaction  
37  
38 to the overall adsorption of ionizable compounds on CNTs is yet to be known, a negative charge  
39  
40 assisted hydrogen bonding (-)CAHB was shown to be particularly strong, which allowed the  
41  
42 adsorbates to overcome the electrostatic repulsion from CNTs. Li and coauthors (2013)<sup>11</sup>  
43  
44 investigated three ionizable aromatic compounds and showed that all three aromatic compounds  
45  
46 with a carboxyl functional group can form (-)CAHB with -COOH on CNT surface. Phthalic  
47  
48 acid containing one benzene ring and two carboxyl functional groups displayed the greatest  
49  
50 formation of (-)CAHB, followed by benzoic acid (BA) with one benzene ring and one carboxyl  
51  
52  
53  
54  
55  
56  
57  
58  
59  
60

1  
2  
3 functional group. 2,6-dichloro-4-nitrophenol exhibited the weakest capability to form (-)CAHB,  
4 likely due to the steric hindrance from functional groups next to the carboxyl functional group.  
5  
6 The results suggested that the formation of (-)CAHB is strongly affected by the molecular size  
7  
8 and structure of adsorbates. Another factor affecting the strength of (-)CAHB is the  $pK_a$   
9  
10 difference between H-donor and H-acceptor, with the strength of (-)CAHB reaching the  
11  
12 maximum when the difference of  $pK_a$  becomes zero.<sup>12</sup> A survey on the literature indicated that  
13  
14 the majority of ionizable compounds investigated for the formation of (-)CAHB so far contained  
15  
16 only one benzene ring to the best of the authors' knowledge<sup>13,14</sup>. Detailed studies on the  
17  
18 adsorption of ionizable aromatic compounds with more than one benzene rings to CNTs and the  
19  
20 potential formation of (-)CAHB of the dissociated ions of these compounds with the oxygen  
21  
22 containing functional groups on CNTs surface have not been conducted. Because most ECs  
23  
24 possess relatively more complex structures than the ionizable compounds investigated in the  
25  
26 literature, and previous studies have shown that steric hindrance can be an important factor in the  
27  
28 adsorption process of ionized ECs on CNTs, it is critical to investigate how the molecular size  
29  
30 and additional functional groups affect the adsorption of ionizable compounds on CNTs. Using  
31  
32 several aromatic carboxylic acids as model adsorbates, the objectives of this study were to (1):  
33  
34 investigate the impact of surface functionalization of multi-walled carbon nanotubes (MWNTs)  
35  
36 on the adsorption of aromatic carboxylic acids; and (2) elucidate the impact of molecular size  
37  
38 and additional functional groups on the adsorption of carboxylic acids on MWNTs. The  
39  
40 formation of (-)CAHB was closely examined under both objectives in addition to the overall  
41  
42 adsorption capacity of these compounds on MWNTs due to its potential significance in the  
43  
44 overall adsorption process.  
45  
46  
47  
48  
49  
50  
51  
52  
53  
54  
55  
56  
57  
58  
59  
60

## Materials and Methods

### *Carbon nanotubes*

Three carbon nanotubes used in this study, including graphitized multi-walled carbon nanotubes (G-MWNTs), hydroxyl-functionalized multi-walled carbon nanotubes (OH-MWNTs), and carboxyl-functionalized multi-walled carbon nanotubes (COOH-MWNTs), were all purchased from US Research Nanomaterials, Inc (Houston, TX). All CNTs had higher than 99.9% purity and similar sizes. Their detailed physicochemical properties reported by the vendor are summarized in **Table S1**.

### *Chemicals*

Benzoic acid (BA) was purchased from Fisher scientific (Houston, TX). 2-naphthoic acid (2-NA), 2-anthroic acid (2-AA) and 3-hydroxy-2-naphthoic acid (3-OH-2-NA) were obtained from Alfa Aesar (Tewksbury, MA). 3-amino-2-naphthoic acid (2-NH<sub>2</sub>-2-NA) was bought from CHEM-IMPEX INT'L INC (Wood Dale, IL) and 3-methoxy-2-naphthoic acid (3-CH<sub>3</sub>O-2-NA) was obtained from TCI (Portland, OR). The molecular structures of these chemicals, as well as their important physicochemical properties such as their octanol-water partitioning coefficient ( $\log K_{ow}$ ) and acid dissociation constant ( $pK_a$ ) are summarized in **Table S2**.

### *Effect of surface functionalization of MWNTs*

Batch experiments were conducted to measure the adsorption isotherms of selected organic acids on MWNTs. For the adsorption of BA, known amount of MWNTs was weighed into 20 mL brown vials. 10 mL of solutions at the concentration range of 0.5-500 mg/L were then added to the vials to mix with MWNTs. HCl or NaOH was used to titrate the pH of the solution to approximately 2.0 and 7.0. The precise values of pH in each vial was recorded with a



1  
2  
3 pH meter. To ensure a reasonable ratio of BA in the liquid and solid phase after adsorption,  
4  
5 different amounts of MWNTs were mixed with different concentrations of BA. Specifically, 5  
6  
7 mg of MWNTs was used for the lowest concentrations (0.5 and 5 mg/L), 10 mg of MWNTs was  
8  
9 used for intermediate concentrations (50 and 200 mg/L) and 15 mg of MWNTs was used for the  
10  
11 highest concentration (500 mg/L). The mixtures were first sonicated for 8 hours in a bath  
12  
13 sonicator (EMERSON, Houston, TX) and then were placed on a shaker table with 120 rpm for 7  
14  
15 days at ambient temperature ( $23 \pm 1^\circ\text{C}$ ) to reach equilibrium. Afterwards, the mixtures were  
16  
17 centrifuged at 3,000 rpm for 20 mins and the pH in the supernatant was measured again with a  
18  
19 pH meter. The concentration of BA or benzoate ( $\text{BA}^-$ ) in the filtrate was quantified with a Perkin  
20  
21 Elmer UV-*vis.* spectrometer at the wavelength from 200 nm to 800 nm. Three replicates were  
22  
23 prepared for each treatment and the adsorption isotherms were measured similarly for all three  
24  
25 MWNTs: G-MWNTs, OH-MWNTs and COOH-MWNTs.  
26  
27  
28  
29  
30

### 31 *Effect of molecular size*

32  
33

34 Three compounds with increasingly larger molecular size: benzoic acid (BA), 2-  
35  
36 naphthoic acid (2-NA) and 2-anthroic acid (2-AA), **Table S2**, were used in this study to probe  
37  
38 the effect of molecular size on the adsorption of ionizable compounds on G-MWNTs and  
39  
40 COOH-MWNTs at pH 7.0 (for BA and 2-NA) or 10.0 (for 2-AA). pH 10.0 was used for 2-AA  
41  
42 due to its low solubility. pH was raised to around 10.0 to fully deprotonate 2-AA so that  
43  
44 relatively higher initial liquid concentration can be obtained. The adsorption isotherms were  
45  
46 determined exactly the same as described above for BA. The initial concentrations used for these  
47  
48 compounds ranged from 0.5 to 50 mg/L and three replicates were prepared for each  
49  
50  
51  
52  
53  
54  
55  
56  
57  
58  
59  
60

### 55 *Effect of molecular structure*

To evaluate the effect of molecular structure on the adsorption of ionizable compounds, three naphthoic acids with additional functional groups including 3-methoxy-2-naphthoic acid (3-CH<sub>3</sub>O-2NA), 3-amino-2-naphthoic acid (3-NH<sub>2</sub>-2-NA) and 3-hydroxy-2-naphthoic acid (3-OH-2-NA) were used in this study. Their molecular structure and important properties are also summarized in **Table S2**. The adsorption isotherms of these compounds on G-MWNTs and COOH-MWNTs at around pH 7.0 were measured as described above. The initial concentrations of these compounds ranged from 0.5 to 50 mg/L due to their relatively low solubility. Three replicates were prepared for each concentration.

### ***Model fitting of the adsorption isotherms***

Freundlich model was used to fit the adsorption isotherms of these acids on MWNTs at different pH values because this model has displayed strong capability to fit the adsorption isotherms of various environmental pollutants on CNTs.<sup>6</sup> The Freundlich model is written as:

$$q_e = K_F C_e^{1/n}$$

Where  $q_e$  is the solid concentration of contaminants on MWNTs (mg/Kg),  $C_e$  is the liquid concentration of contaminants at equilibrium (mg/L),  $1/n$  is a measure of the concentration dependent change in adsorption affinity and  $K_F$  (mg/Kg/(mg/L)<sup>1/n</sup>) is an indicator of adsorption capacity.

### ***Simulation on effects of molecular size and structure on non-charge interactions***

All molecules of interest were tested for non-charge interactions with the surface of MNNTs. An in-house script was developed to capture these interactions using a standard 12/6 Lennard-Jones potential:  $4\epsilon \left[ \left( \frac{\sigma}{r} \right)^{12} - \left( \frac{\sigma}{r} \right)^6 \right]$  for  $r < r_c$  where  $\epsilon$  describes the strength of the interaction and  $\sigma$  is the zero-potential distance.  $\epsilon$  and  $\sigma$  are uniquely assigned to each atom (and

1  
2  
3 geometrically averaged for each pair) based on OPLS-aa forcefield as embedded in LigParGen  
4  
5 OPLS-AA parameter generator.<sup>15,16</sup>  $r_c$  is pair separation distance where the interaction potential  
6  
7 is negligibly small.  
8  
9

## 10 **Results and Discussion**

### 11 *Effects of surface functionalization*

12  
13  
14  
15  
16 The adsorption isotherms of BA and BA<sup>-</sup> at pH ~2.0 and ~7.0 are shown in **Figure 1**.  
17  
18 The pH values were maintained so that the majority of the BA was either fully protonated or  
19 fully deprotonated. As expected, surface functionalization played a significant role in the  
20 adsorption of BA at pH 2.0, with COOH-MWNTs displayed the greatest adsorption, followed by  
21 OH-MWNTs and then G-MNNTs. Due to the presence of benzene rings in both the adsorbent  
22 and adsorbate,  $\pi$ - $\pi$  interactions contributed to the adsorption of BA to MWNTs in addition to the  
23 hydrophobic effect. If these are the only intermolecular forces, the adsorption of BA on these  
24 MWNTs would be smaller in functionalized MWNTs due to the occupation of some adsorption  
25 sites by the functional groups.<sup>17</sup> The stronger adsorption of BA on functionalized MWNTs at pH  
26 2.0 suggested the existence of other intermolecular forces. Hydrogen bonding can be formed  
27 between oxygen and hydrogen atoms on the carboxyl functional group of BA and the functional  
28 group on MWNTs. The greater adsorption of BA on COOH-MWNTs was attributed to the  
29 formation of a dimer, or a double hydrogen bonding formed between the carboxyl functional  
30 groups on BA and MWNTs. Only one hydrogen bonding can be formed between BA and the OH  
31 group on OH-MWNT, resulting in greatest adsorption of BA on COOH-MWNTs.  
32  
33  
34  
35  
36  
37  
38  
39  
40  
41  
42  
43  
44  
45  
46  
47  
48  
49  
50

51 BA is predominantly protonated at pH 2.0 and deprotonated at pH 7.0. Since the dissociated  
52 form is much more hydrophilic than the neutral form, the hydrophobic effect is significantly  
53 weaker at pH 7.0. As shown in **Figure 1**, BA is more adsorptive on G-MWNTs at pH 2.0 than at  
54  
55  
56  
57  
58  
59  
60

1  
2  
3 pH 7.0, consistent with the much higher octanol-water partitioning coefficient ( $K_{ow}$ ) of BA than  
4 benzoate ( $BA^-$ ). The result suggest that the hydrophobic effect is an important mechanism for the  
5 adsorption of BA on CNTs. Interestingly, BA displayed greater adsorption on the functionalized  
6 MWNTs at pH 7.0 than at pH 2.0, suggesting that other intermolecular forces contributed to the  
7 adsorption of  $BA^-$  on functionalized MWNTs at pH 7.0. The difference between the adsorption of  
8  $BA^-$  and BA was greatest for OH-MWNTs. Due to the importance of electrostatic forces, we first  
9 measured the point of zero charge (PZC) of different MWNTs through titration and the results  
10 revealed that the PZC of G-MWNTs was around 2.3 while the PZC of both functionalized MWNTs  
11 was around 10.0. At around pH 7.0, the functionalized MWNTs are both positively charged while  
12 the G-MWNTs are negatively charged. Because  $BA^-$  carries a negative charge, the electrostatic  
13 attraction between  $BA^-$  and both functionalized MWNTs contributed to the adsorption of  $BA^-$  on  
14 these CNTs. However, electrostatic attractions might not be the only force leading to higher  
15 adsorption of  $BA^-$  onto functionalized MWNTs because both functionalized MWNTs have similar  
16 PZC, yet the adsorption of benzoate on OH-MWNTs is greater.

17  
18  
19  
20  
21  
22  
23  
24  
25  
26  
27  
28  
29  
30  
31  
32  
33  
34  
35  
36  
37  
38  
39  
40  
41  
42  
43  
44  
45  
46  
47  
48  
49  
50  
51  
52  
53  
54  
55  
56  
57  
58  
59  
60  
Previous studies have shown that dissociated aromatic carboxylates can form a particularly  
strong charge-assisted hydrogen bonding ((-)CAHB) with oxygen-containing functional groups on  
CNTs [11]. The formation of (-)CAHB requires proton exchange with water molecules so that a  
strong hydrogen bond between the oxygen on the carboxyl functional group on  $BA^-$  and the oxygen  
on the CNT surface can be formed as  $O^- \dots H^+ \dots O^-$ . A direct consequence of the water molecule  
splitting is the release of hydroxide ions ( $OH^-$ ) during the adsorption process. We measured the  
hydroxide ion release during the adsorption of  $BA^-$  on all CNTs following the method reported  
earlier.<sup>14</sup> Briefly, the released hydroxide ion was calculated as the sum of the  $OH^-$  that caused the  
pH change in solution and the  $OH^-$  consumed by CNTs. The  $OH^-$  consumption by the two

1  
2  
3 functionalized MWNTs was estimated from the titration curves shown in **Figure S1**. The release  
4 of hydroxide ion from G-MWNTs was insignificant and is not shown, however, much greater  
5 hydroxide ions were released from the COOH-CNTs and OH-CNTs, **Figure 2**, confirming the  
6 occurrence of the (-)CAHB between  $\text{BA}^-$  and the O-containing functional groups on CNTs. The  
7 greater release of  $\text{OH}^-$  from OH-MWNTs is consistent with the stronger adsorption of  $\text{BA}^-$  on this  
8 adsorbent. To compare the (-)CAHB formation potential of  $-\text{OH}$  and  $-\text{COOH}$ , we normalized the  
9  $\text{OH}^-$  based on the density of these functional groups on the functionalized MWNTs, **Table S1**.  
10 After the normalization, the curves of  $\text{OH}^-$  release from both functionalized MWNTs essentially  
11 overlapped, indicating that both functional groups display similar capability to form (-)CAHB with  
12 benzoate. In summary, our results indicate that the adsorption of BA on functionalized MWNTs  
13 is stronger than G-MWNTs at both pH 2.0 and 7.0 for different reasons. The formation of hydrogen  
14 bonding between BA and O-containing functional groups on MWNTs overcomes the reduced  
15 adsorption sites and leads to greater adsorption of BA on functionalized MWNTs at pH 2.0. At pH  
16 7.0, the greater adsorption of  $\text{BA}^-$  on functionalized MWNTs is mainly attributed to the  
17 electrostatic attraction and the formation of (-)CAHB between  $\text{BA}^-$  and the functional groups on  
18 MWNTs.

### 39 ***Effects of molecular size***

40  
41  
42 To understand how the molecular size of aromatic carboxylates affect their adsorption on  
43 MWNTs and the formation of (-)CAHB, BA, 2-naphthoic acid (2-NA) and 2-anthroic acid (2-AA)  
44 were used as representative ionizable compounds with increasing number of benzene rings. Their  
45 adsorption isotherms on both G-MWNTs and COOH-MWNTs at pH 7.0 or 10.0 are shown in  
46 **Figure 3**. 2-NA displayed the highest adsorption, followed by 2-AA and then BA on G-MWNTs.  
47 It is well recognized that  $K_{ow}$  values of neutral compounds tabulated in **Table S2** are not good

indicators of the adsorption behavior of the dissociated ions.<sup>18</sup> Instead, pH-dependent  $K_{ow}$ , or  $D_{ow}$ , should be used to gauge the importance of hydrophobic effects of ionizable compounds on their adsorption to CNTs.<sup>19</sup>  $D_{ow}$  can be estimated using the following equation:

$$D_{ow} = f_{HA}K_{ow}^{HA} + f_{A^-}K_{ow}^{A^-}$$

where  $f_{HA}$  refers to the fraction of neutral acids and  $f_{A^-}$  refers to the fraction of dissociated acids.  $K_{ow}^{HA}$  and  $K_{ow}^{A^-}$  refer to the octanol water partitioning coefficient of neutral acids and their conjugate bases, respectively. The fractions of neutral acids and their bases at different pH conditions are calculated following the two equations below:

$$f_{HA} = \frac{1}{(1 + 10^{pH - pKa})}$$

and

$$f_{A^-} = \frac{1}{(1 + 10^{pKa - pH})}$$

Plugging the actual pH of 6.85 (~7.0) for BA and 2-NA or 9.57 (~10.0) for 2-AA, and using  $K_{ow}$  values listed in **Table S2** for neutral compounds and literature data for the  $K_{ow}$  of dissociated acids [19],  $D_{ow}$  of these three compounds are estimated as: -0.041, 0.201, and 0.123 for BA, 2-NA and 2-AA respectively, consistent with their adsorption on G-WMNTs. The  $K_{ow}$  of  $BA^-$  was cited from the literature<sup>19</sup> and the  $K_{ow}$  of other two dissociated ions were estimated using the data reported in the same study. The results suggested that even though the dissociated forms are much more hydrophilic than their neutral compounds, the hydrophobic effect remains an important intermolecular force for the adsorption of ionized compounds on G-MWNTs. In addition to the hydrophobic force, electrostatic repulsion between G-MWNTs (PZC=2.3) and these negatively charged compounds also limited their adsorption and the repulsion would be strongest for 2-AA due to the higher extent of dissociation of this compound at pH 10.0.

1  
2  
3 A comparison of the adsorption isotherms of these compounds on COOH-MWNTs and  
4 G-MWNTs indicates that the adsorption of these three compounds followed a different order,  
5 specifically, the adsorption of BA<sup>-</sup> onto COOH-MWNTs was greatly improved but the  
6 adsorption of 2-AA<sup>-</sup> was significantly inhibited. As mentioned earlier, the PZC of COOH-  
7 MWNTs is around 10.0. At pH 7.0, electrostatic attraction would increase the adsorption of BA<sup>-</sup>  
8 and 2-NA<sup>-</sup>, and this enhanced adsorption could compensate for the lost adsorption sites due to  
9 COOH functional group. However, the markedly improved adsorption of BA<sup>-</sup> at pH 7.0  
10 compared to that of 2-NA<sup>-</sup> suggested that other molecular forces might also play a role. As  
11 indicated earlier, (-)CAHB was formed between BA<sup>-</sup> and COOH-MWNTs which contributed to  
12 the adsorption of BA<sup>-</sup> to COOH-MWNTs. To determine whether (-)CAHB was also formed  
13 between COOH-MWNTs with 2-NA<sup>-</sup> and 2-AA<sup>-</sup> at the tested pH conditions, the hydroxide ion  
14 release was similarly calculated. Surprisingly, the release of OH<sup>-</sup> was insignificant for both 2-  
15 NA<sup>-</sup> and 2-AA<sup>-</sup> even though they possess fairly similar structures as BA<sup>-</sup>. The formation of  
16 (-)CAHB between BA<sup>-</sup> and COOH-MWNTs agrees with the much stronger adsorption of BA<sup>-</sup> on  
17 COOH-MWNTs than other two acids. Because the adsorption of 2-AA was performed at pH  
18 10.0, close to the PZC of COOH-MWNTs, there was no electrostatic attraction between 2-AA<sup>-</sup>  
19 and almost neutral COOH-MWNTs. The absence of the electrostatic attraction and the inability  
20 to form (-)CAHB with the -COOH functional group on CNTs, as well as the lost adsorption sites  
21 to -COOH functional group, together resulted in the much lower adsorption of 2-AA<sup>-</sup> on COOH-  
22 MWNTs at pH 10.0. While previous studies have shown that additional functional groups next to  
23 the carboxyl functional group could sterically hinder the formation of (-)CAHB, this is the first  
24 time to demonstrate that additional benzene rings in the molecular structure significantly lowered  
25 the capability of aromatic carboxylates to form (-)CAHB with O-containing functional groups on  
26  
27  
28  
29  
30  
31  
32  
33  
34  
35  
36  
37  
38  
39  
40  
41  
42  
43  
44  
45  
46  
47  
48  
49  
50  
51  
52  
53  
54  
55  
56  
57  
58  
59  
60

MWNTs. Why additional benzene rings significantly inhibited the formation of (-)CAHB is yet to be fully understood. It is possible that additional benzene rings in the molecular structure significantly changed the orientation of these molecules when they approached the surface of CNTs, minimizing the contact of carboxyl functional groups with the functional groups on CNTs and consequently lowering the formation of (-)CAHB.

To gain more insights into the size effect of aromatic carboxylates on their adsorption, we investigated the influences of aromatic ring multiplicity of neutral BA, 2-NA and 2-AA on their adsorption on individual MWNTs through molecular simulation. The neutral forms were used to avoid the confounding effect of electrostatics. A no-defect 3-layer CNT was developed with concentric armchair chiralities of 5, 10, and 15, which translate into a radii difference of 3.4 Å, in accordance with the recommended value for MWNTs.<sup>20</sup> The normal vector to the benzene ring is selected to describe the three dimensional orientations by evaluating the angle this vector makes with the tube longitudinal axis,  $\phi$ , as well as the angle its cross-sectional projection makes with the tube radial vector,  $\theta$ . Energy minima are sought by screening orientations at a resolution of 2 degrees, and at center of mass clearance from tube in increments of 0.05 Å. As shown in the distance-potential relationships in **Figure 4**, Increase in number of aromatic rings from BA to 2-NA and then 2-AA provided a clear advantage in adsorption potential. BA and 2-NA adhered best at face flat orientation: a  $\phi$  angle close to 90° and a  $\theta$  angle close to either 0° or 180°. While this configuration provides very good  $\pi$ - $\pi$  stacking opportunity, 2-AA, owing to its larger size, deviated from this orientation as it experienced the curved substrate surface much less planar than BA and 2-NA do, supporting our experimental observation that additional benzene rings in 2-AA<sup>-</sup> altered the attachment orientation in adsorption. The result also supports the



1  
2  
3 observed adsorption patterns on G-MWNTs because additional benzene ring in 2-NA enhanced  
4  
5 the hydrophobic effect of this compound.  
6  
7

### 8 *Effects of molecular structure*

9

10  
11 The adsorption isotherms of 2-NA, 3-methoxy-2-naphthoic acid (3-CH<sub>3</sub>O-2NA), 3-  
12 amino-2-naphthoic acid (3-NH<sub>2</sub>-2-NA) and 3-hydroxy-2-naphthoic acid (3-OH-2-NA) on G-  
13 MWNTs and COOH-MWNTs at pH 7.0-8.5 are shown in **Figure 5**. All three compounds with  
14  
15 MWNTs and COOH-MWNTs at pH 7.0-8.5 are shown in **Figure 5**. All three compounds with  
16  
17 an additional functional group are more hydrophilic than 2-NA, likely due to the additional  
18  
19 hydrogen bond formation capacity between water molecules and the additional functional  
20  
21 groups. The presence of -NH<sub>2</sub> decreased the acidity of 2-NA but other two functional groups  
22  
23 increased the acidity, **Table S1**.  
24  
25  
26

27  
28 Based on the adsorption isotherms, 3-NH<sub>2</sub>-2-NA displayed the strongest adsorption on G-  
29 MWNTs followed by 2-NA, then 3-OH-2-NA and 3-CH<sub>3</sub>O-2-NA. An estimation of  $D_{ow}$  of these  
30  
31 acids following a similar approach are around 0.188, 0.201, -0.206 and -0.356, respectively,  
32  
33 roughly consistent with the observed order of their adsorption, indicating that hydrophobic effect  
34  
35 remained an important molecular force for the adsorption of ionizable compounds on MWNTs.  
36  
37 At pH 7, the G-MWNTs were negatively charged, therefore, electrostatic repulsion would reduce  
38  
39 the adsorption of all four compounds because all ionized compounds are negatively charged in  
40  
41 this study. However, the pKa of 3-NH<sub>2</sub>-2-NA is much larger than other three compounds as  
42  
43 shown in **Table S2**, therefore, a larger fraction of this compound remained as neutral even at  
44  
45 around pH 7. Consequently, electrostatic repulsion would be the weakest for this compound,  
46  
47 consistent with the greatest adsorption of 3-NH<sub>2</sub>-2-NA<sup>-</sup> on G-MWNTs. The results suggest that  
48  
49 hydrophobic effect and electrostatic interactions are two dominant forces for the adsorption of  
50  
51 these compounds on G-MWNTs. We further investigated the effect of functional groups on the  
52  
53  
54  
55  
56  
57  
58  
59  
60

1  
2  
3 adsorption of 2-NA on individual MWNTs through molecular simulation. As shown in **Figure**  
4  
5 **4**, functional group attachment on 2-NA provided an appreciable advantage in adsorption  
6  
7 potential. Particularly, amine and hydroxyl groups resulted in comparable energy minima.  
8  
9 However, there is nearly 5% more adsorbate-adsorbent pair count within the LJ influence region  
10  
11 when an amino group is attached. This attests to the distance and atomic configuration sensitivity  
12  
13 of the attractive and repulsive components of the LJ potential. A methoxy attachment afforded  
14  
15 the smallest energy minima than either the amine or hydroxyl groups. The results of the  
16  
17 simulation are consistent with our experimental observation on the adsorption order of these  
18  
19 compounds on G-MWNTs. It should be cautioned that the calculation scheme adopted here  
20  
21 exaggerates the non-bonded interactions because the role of water molecules in the adsorption  
22  
23 process was not considered in the simulation. Nevertheless, the results shed important light on  
24  
25 the effect of functional groups in a molecular structure on their adsorption affinity to CNTs.  
26  
27  
28  
29  
30

31 The adsorption of these compounds on COOH-MWNTs follows a similar order, but  
32  
33 relatively lower adsorption of 2-NA was observed as discussed above. The calculation of  
34  
35 hydroxide ion release from the adsorption of these compounds on COOH-MWNTs indicates that  
36  
37 (-)CAHB was minimal in the adsorption of selected compounds at pH 7.0, consistent with  
38  
39 previous publications that the steric hindrance plus the additional benzene ring on the molecular  
40  
41 structure prohibited the formation of (-)CAHB. As indicated earlier, the  $\Delta pK_a$  between H-donor  
42  
43 and H-acceptor dictates the strength of (-)CAHB. It is possible that increasing structural  
44  
45 complexity of adsorbates changes the attachment orientation of these adsorbates, making it  
46  
47 more difficult to form (-)CAHB between carboxyl groups on the carboxylic acids and MWNT  
48  
49 surfaces, resulting in much weaker (-)CAHB for these compounds. Additional investigation is  
50  
51 needed to confirm this hypothesis.  
52  
53  
54  
55  
56  
57  
58  
59  
60

### *Summary and concluding remarks*

Over the past decade, numerous efforts have been dedicated to understanding the fate, occurrence and removal of ECs. The adsorption of emerging ionizable compounds on environmental surfaces plays a significant role in their fate and transport in the environment. Alternatively, the adsorption process also provides an effective pathway to remove these ECs from the environment. Consequently, it is imperative to understand the underlying adsorption mechanisms of ionizable compounds on different environmental surfaces including carbonaceous surfaces.

The major roles of hydrophobicity and electrostatic interactions in the adsorption of ionizable compounds on MWNTs are clearly demonstrated. In addition, we applied molecular simulation to evaluate the adsorption orientation of different molecules on MWNT surfaces and showed the connections of the adsorption attachment orientation and the chemistry occurred on the solid liquid interface such as the formation of (-)CAHB, as summarized in **Figure 6A** and **Figure 6B**. Solution chemistry, predominantly the solution pH, is a significant factor in the adsorption of ionizable compounds and the pH-dependent octanol-water partitioning coefficients provides a better indicator on the extent of hydrophobicity, an intermolecular effect modified by the molecular size enlargement and attachment moieties, as summarized in **Figures 6C** and **6D**.

Because many ECs have more complex molecular structures than the molecular probes used to investigate the mechanisms of (-)CAHB in the literature, its significance for the adsorption of large, more complex emerging ionizable compounds on carbon nanotubes is yet to be confirmed. What is interesting from this study is that more aromatic rings confer a van der Waals advantage on neutral molecules, but once deprotonation is in effect less number of aromatic rings corresponded with better (-)CAHB performance. The results suggest that

1  
2  
3 (-)CAHB may not be a significant factor in the adsorption of more complex emerging ionizable  
4  
5 compounds. While this study has shed significant light on the adsorption of ionizable compounds  
6  
7 on MWNTs, the energetic calculations were performed in an ideal environment. They are useful  
8  
9 guides for full-fledged simulations, but simulations treating the solvent water and adsorbent  
10  
11 molecules at experimentally relevant concentrations and ionization conditions, as well as more  
12  
13 detailed studies involving competitive adsorption in more realistic environmental conditions are  
14  
15 needed in future studies.<sup>21</sup> Advancement in the materials science to modify the properties of  
16  
17 carbonaceous materials may further enhance their performance in the removal of environmental  
18  
19 contaminants. Two recent studies showed that inclusion of heteroatoms such as nitrogen and  
20  
21 phosphorous in the carbon structures of graphene enhanced the electron donor-acceptor  
22  
23 relationship between the adsorbent and various environmental pollutants, significantly increasing  
24  
25 their adsorption capacity.<sup>22,23</sup> Overall, the results reported here expanded the core body of  
26  
27 knowledge necessary to design efficient *in-situ* organic contaminant removal by carbonaceous  
28  
29 materials.  
30  
31  
32  
33  
34  
35  
36  
37

38 Supplementary Information Included.

### 39 40 **Acknowledgements**

41  
42  
43 Xingmao Ma and Saikat Talapatra acknowledge the financial support from NSF through the  
44  
45 project CHE-1623238. Iskinder Arsano and Mesfin Tsige acknowledge NSF support through  
46  
47 grant #CHE-1665284.

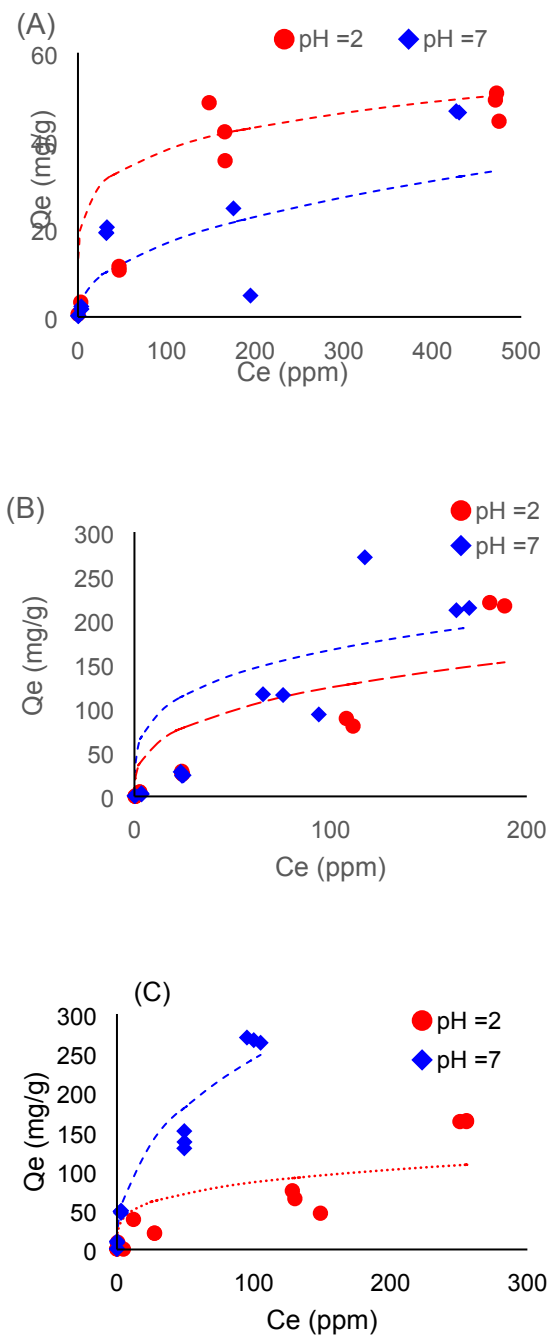
### 48 **References**

49  
50  
51 [1] Petri, B., Barden, R., Kasprzyk-Hordern, B. A review on emerging contaminants in  
52  
53 wastewaters and the environment: current knowledge, understudied areas and recommendations  
54  
55 for future monitoring. *Water Res.*, 2015, 72, 3-27.  
56  
57

- 1  
2  
3 [2] Hughes, S. R., Kay, P., Brown, L. E. Global synthesis and critical evaluation of  
4 pharmaceutical data sets collected from river systems. *Environ. Sci. Technol.*, 2013, 47, 661-677.  
5  
6  
7  
8 [3] Rizzo, L., Malato, S., Antakyali, D., Beretsou, V. G., Dolic, M. B., Gernjak, W., Heath, E.,  
9 Ivancev-Tumbas, I., Karoolia, P., Lado Ribeiro, A. R., Mascolo, G., McArdell, C. S., Schaar, H.,  
10 Silva, A. M. T., Fatta-Kassinos, D. Consolidated vs new advanced treatment methods for the  
11 removal of contaminants of emerging concern from urban wastewater. *Sci. Total Environ.* , 2019,  
12 655, 986-1008.  
13  
14  
15 [4] Sophia A. C., Lima, E. C. Removal of emerging contaminants from the environment by  
16 adsorption. *Ecotoxicol. Environ. Saf.*, 2018, 150, 1-17.  
17  
18  
19 [5] Ma, X., Anand, D., Zhang, X., Talapatra, S. Adsorption and desorption of chlorinated  
20 compounds from pristine and thermally treated multiwalled carbon nanotubes. *J. Phys. Chem. C.*,  
21 2011, 115, 4552-4557.  
22  
23  
24 [6] Yang, K. and Xing, B. Adsorption of organic compounds by carbon nanomaterials in aqueous  
25 phase: Polanyi theory and its application. *Chem. Rev.*, 2010, 110, 5989-6008.  
26  
27  
28 [7] Ma, X., Agarwal, S. Adsorption of emerging ionizable contaminants on carbon nanotubes:  
29 advancements and challenges. *Molecules*, 2016, 21, 628.  
30  
31  
32 [8] Kah, M., Sigmund, G., Xiao, F., Hofmann, T. Sorption of ionizable and ionic organic  
33 compounds to biochar, activated carbon and other carbonaceous materials. *Water Res*, 2017, 124,  
34 673-692.  
35  
36  
37 [9] Tang, H., Zhao, Y., Yang, X., Liu, D., Shan, S., Cui, F., Xing, B. Understanding the pH-  
38 dependent adsorption of ionizable compounds on graphene oxide using molecular dynamics  
39 simulations. *Environ. Sci.: Nano.*, 2017, 4, 1935-1943.  
40  
41  
42  
43  
44  
45  
46  
47  
48  
49  
50  
51  
52  
53  
54  
55  
56  
57  
58  
59  
60

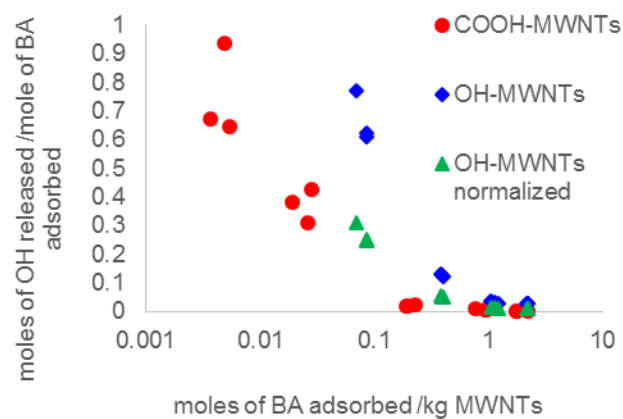
- 1  
2  
3 [10] Zhang, K., Chen, B., Mao, J., Zhu, L., Xing, B. Water clusters contributed to molecular  
4 interactions of ionizable organic pollutants with aromatized biochar via  $\pi$ -PAHB: sorption  
5 experiments and DFT calculations. *Environ. Poll.*, 2018, 240, 342-352.  
6  
7  
8  
9  
10 [11] Li, X., Pignatello, J. J., Wang, Y., Xing, B. New insight into adsorption mechanism of  
11 ionizable compounds on carbon nanotubes. *Environ. Sci. Technol.*, 2013, 47, 8334-8341.  
12  
13  
14  
15 [12] Gilli, P., Pretto, L., Bertolasi, V., Gilli, G. Predicting hydrogen-bond strengths from acid-  
16 base molecular properties. The pK<sub>a</sub> slid rule: toward the solution of a long-lasting problem. *Acc.*  
17  
18  
19  
20  
21  
22  
23 [13] Li, X., Gamiz, B., Wang, Y., Pignatello, J. J., Xing, B. Competitive sorption used to probe  
24 strong hydrogen bonding sites for weak organic acids on carbon nanotubes. *Environ. Sci.*  
25  
26  
27  
28  
29  
30  
31 [14] Ni, J., Pignatello, J. J., Xing, B. Adsorption of aromatic carboxylate ions to black carbon  
32 (biochar) is accompanied by proton exchange with water. *Environ. Sci. Technol.*, 2011, 45, 9240-  
33  
34  
35  
36  
37  
38 [15] Jorgensen, W. L., Tirado-Rives, J.. Chemical theory and computation special feature:  
39 potential energy functions for atomic-level simulations of water and organic and biomolecular  
40 systems. *Proc. Natl. Acad. Sci. USA*, 2005, 102, 6665-6670.  
41  
42  
43  
44  
45 [16] Dodda, L.S., Cabeza de Vaca, I., Tirado-Rives, J., Jorgensen, W. L. LigParGen web server:  
46 an automatic OPLS-AA parameter generator for organic ligands. *Nucleic Acids Res.* 2017, 45  
47  
48  
49  
50  
51  
52  
53  
54  
55  
56  
57  
58  
59  
60

- 1  
2  
3 [17] Wei, J., Sun, W., Pan, W., Yu, X., Sun, G., Jiang, H. Comparing the effects of different  
4 oxygen-containing functional groups on sulfonamides adsorption by carbon nanotubes:  
5 experiments and theoretical calculation. *Chem. Eng. J.*, 2017, 312, 167-179.  
6  
7  
8  
9  
10 [18] Sigmund, G., Sun, H., Hofmann, T., Kah, M. Predicting the sorption of aromatic acids to  
11 nanocarbonized and carbonized sorbents. *Environ. Sci. Technol.*, 2016, 50, 3641-3648.  
12  
13  
14 [19] Li, H., Cao, Y., Zhang, D., Pan, B. pH-dependent Kow provides new insights in  
15 understanding the adsorption mechanisms of ionizable organic chemicals on carbonaceous  
16 materials. *Sci. Total Environ.*, 2018, 618, 269-275.  
17  
18  
19  
20  
21 [20] Peigney, A., Laurent, C., Flahaut, E., Bacsá, R. P., Rousett, A. Specific surface area of  
22 carbon nanotubes and bundles of carbon nanotubes. *Carbon*, 2001, 39(4), 507-514.  
23  
24  
25  
26  
27 [21] Ma, X. Wang, C. Impact of the physiochemical properties of chlorinated solvents on the  
28 sorption of trichloroethylene to the roots of *Typha latifolia*. *Environ. Poll.*, 2009, 157, 1019-  
29 1023.  
30  
31  
32  
33  
34 [22] Wang, W., Gong, Q., Chen, Z., Wang, W. D., Huang, Q., Song, S., Chen, J., Wang, X.  
35 Adsorption and competition investigation of phenolic compounds on the solid-liquid interface of  
36 three dimensional foam-like graphene oxide. *Chem. Eng. J.*, 2019, 378, 122085.  
37  
38  
39  
40  
41 [23] Wang, W., Wang, X., Xing, J., Gong, Q., Wang, H., Wang, J., Chen, Z., Ai, Y., Wang, X.  
42 Multi-heteroatom doped graphene-like carbon nanospheres with 3D inverse opal structure: a  
43 promising biosphenol-A remediation material. *Environ. Sci: Nano.*, 2019, 6, 809-819.  
44  
45  
46  
47  
48  
49  
50  
51  
52  
53  
54  
55  
56  
57  
58  
59  
60

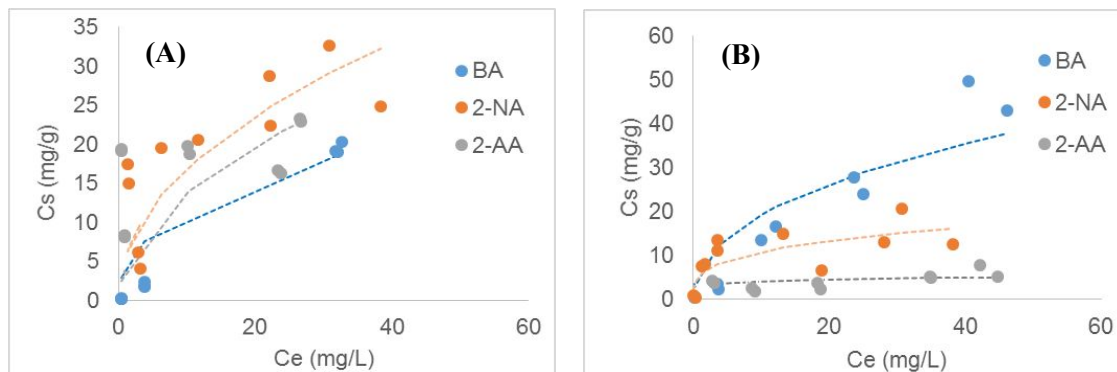


**Figure 1:** The adsorption isotherms of benzoic acid on three different types of carbon nanotubes at pH 2.0 and 7.0, (A) G-MWNTs; (B) OH-MWNTs, and (C) COOH-MWNTs. Dotted lines are fittings curves with Freundlich model.

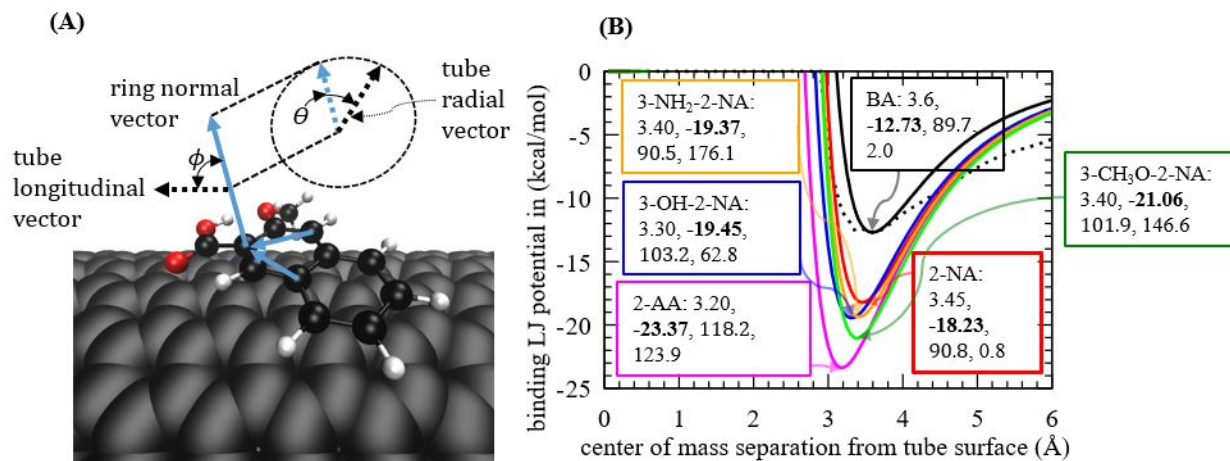




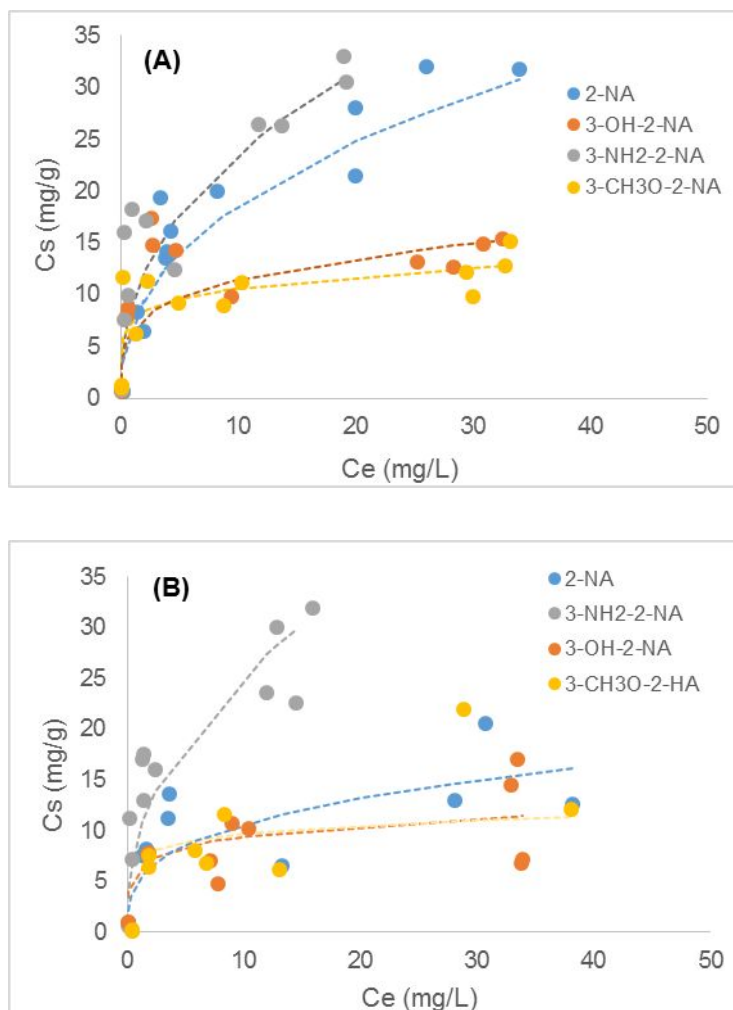
**Figure 2:** Moles of hydroxide ion release per mole of benzoic acid (BA) adsorbed on COOH- or OH- functionalized multi-walled carbon nanotubes. Green triangles are OH<sup>-</sup> released from the adsorption of BA on OH-MWNTs normalized by the percentage of -OH functional groups on MWNTs.



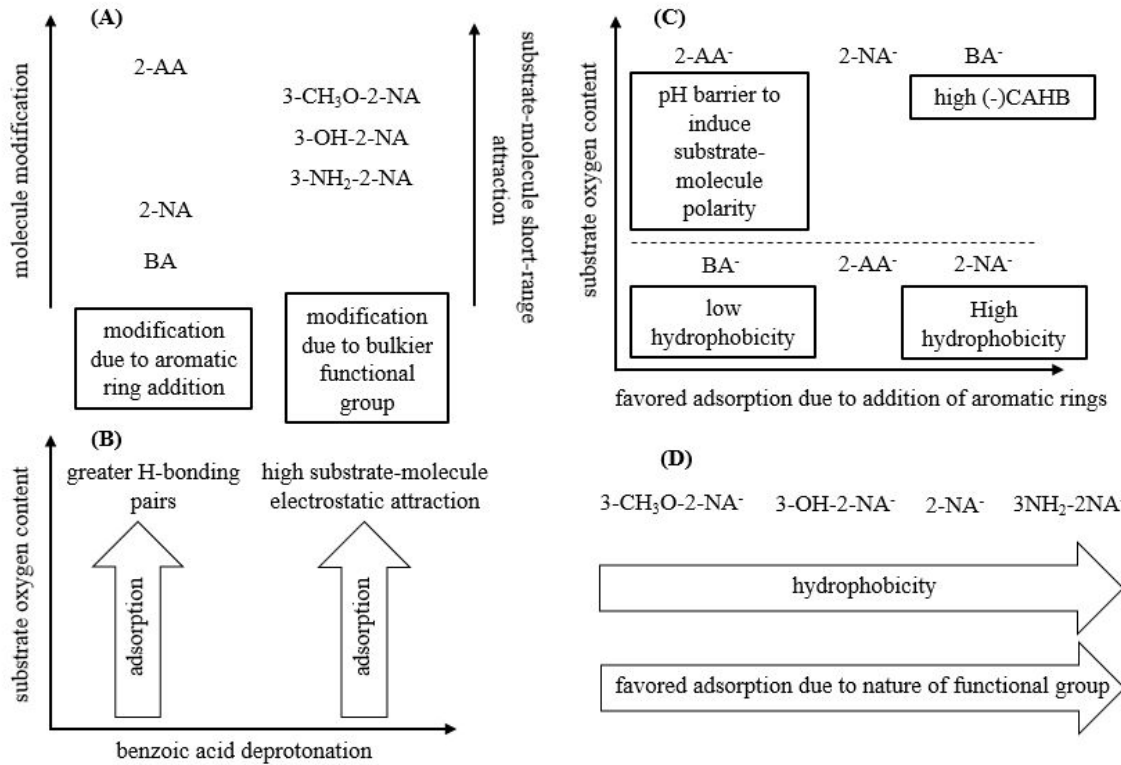
**Figure 3:** The adsorption isotherms of BA, 2-NA and 2-AA on graphitized MWNTs (A) and carboxyl functionalized MWNTs (COOH-MWNTs) (B) at pH  $\sim 7.0$  or  $\sim 10.0$ . The dotted lines are Freundlich model fittings. BA: benzoic acid; 2-NA: 2-naphthoic acid; 2-AA: 2-anthoic acid. Dotted lines represent the fitting curves of Freundlich modeling.



**Figure 4:** (A) Schematic describing the ring-normal orientation vector as a cross product of two in-plane vectors on the aromatic ring common to the 6 contaminants studied.  $\phi$ : angle between ring normal vector and longitudinal axis.  $\theta$ : angle between cross-sectional projection of ring normal vector and radial axis. (B) Minimum individual adsorption potential on a model no-defect G-MWNT surface. Numbers in the boxes are, in order, center of mass clearance from tube in angstroms, adsorption potential in kcal/mol,  $\phi$  in degrees, and  $\theta$  in degrees. The dotted line is an example demonstration from the minimum energy sample space where minimum energy is extracted at each separation distance increment. BA (black): benzoic acid; 2-NA (red): 2-naphthoic acid; 2-AA (magenta): 2-anthroic acid, 3-OH-2-NA (blue): 3-hydroxyl-2-naphthoic acid, 3-NH<sub>2</sub>-2-NA (orange): 3-amino-2-naphthoic acid, 3-CH<sub>3</sub>O-2-NA (green): 3-methoxyl-2-naphthoic acid.



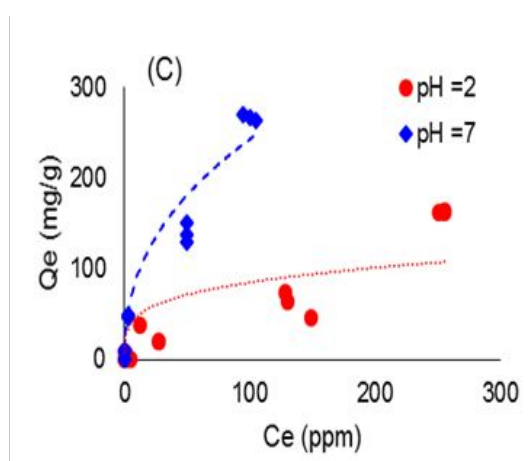
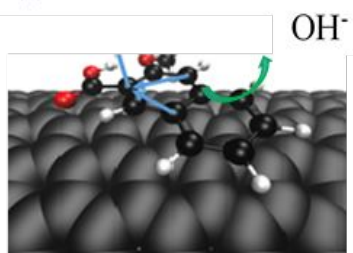
**Figure 5:** Adsorption isotherms of 2-naphthoic acids with different functional groups on G-MWNTs (A) and COOH-MWNTs (B). 2-NA:2-naphthoic acid, 3-OH-2-NA: 3-hydroxyl-2-naphthoic acid, 3-NH<sub>2</sub>-2-NA: 3-amino-2-naphthoic acid, 3-CH<sub>3</sub>O-2-NA: 3-methoxyl-2-naphthoic acid.



**Figure 6:** Predominant parameters driving adsorption. Adsorption of neutral contaminants on model G-MWNT (A); adsorption effects of deprotonating neutral contaminants using the example of BA (B); and adsorption of majority ionized contaminants (C) and (D). BA: benzoic acid; 2-NA: 2-naphthoic acid; 2-AA: 2-anthroic acid, 3-OH-2-NA: 3-hydroxyl-2-naphthoic acid, 3-NH<sub>2</sub>-2-NA: 3-amino-2-naphthoic acid, 3-CH<sub>3</sub>O-2-NA: 3-methoxyl-2-naphthoic acid.

## Graphical Abstract

Hydrophobic effect  
Electrostatic interactions  
 $\pi$ - $\pi$  stacking  
(-)CAHB



Surface functionalization and molecular properties affect the formation of (-)CAHB and the overall adsorption of carboxylic acids on MWNTs